Advances in Science and Technology Research Journal

Advances in Science and Technology Research Journal, 2025, 19(8), 313–331
https://doi.org/10.12913/22998624/205691
ISSN 2299-8624, License CC-BY 4.0

Received: 2025.05.05
Accepted: 2025.06.15
Published: 2025.07.01

Influence of speed and heat input of the pulsed-arc welding process on the structure formation of Al-Mg-Mn aluminum alloy joints

Volodymyr Korzhyk[1,2], Shiyi Gao[1*], Vladyslav Khaskin[1,2], Yevhenii Illiashenko[1,2], Andrii Grynyuk[2], Andriy Alyoshin (Junior)[2], Oleksandr Bushma[2], Xinxin Wang[1], Yanchao Hu[2], Guirong[2]

[1] China-Ukraine Institute of Welding, Guangdong Academy of Sciences, Guangdong Provincial Key Laboratory of Material Joining and Advanced Manufacturing, Guangzhou, 510650, China

[2] E.O. Paton Electric Welding Institute, National Academy of Sciences of Ukraine, 03150, Kazymyr Malevych Str., 11, Kyiv, Ukraine

* Corresponding author's e-mail: meshiyigao@163.com

ABSTRACT

This paper establishes the trends in structure formation of 4 mm thick 1561 aluminum alloy welded joints, depending on changes in the parameters of the MIG welding mode on a steel substrate (specifically, the speed and heat input of the process). Welding modes were selected based on the criterion of satisfactory seam formation, and the optimal welding mode was determined based on the criteria of minimizing porosity, grain refinement, and improved mechanical properties. Technological studies have shown that, based on the criterion of satisfactory seam formation with a quality level ranging from C to B according to ISO 10042, it is advisable to select a welding speed between 380 and 600 mm/min with a heat input between 217 and 240 J/mm. Metallographic studies have shown that increasing the MIG welding speed promotes weld grain refinement, decreases their shape factor, and simultaneously increases the number of pores while reducing their size. Mechanical tests demonstrated that increasing the welding speed enhances the mechanical properties of welded joints. Therefore, when using MIG welding of aluminum alloys in industry, it is recommended to increase the speed to 600 mm/min and higher.

Keywords: aluminum alloy, pulsed gas metal arc welding (MIG), parameters, structures, strength.

INTRODUCTION

Reducing the weight and material consumption of vehicles and industrial products has consistently been a significant concern [1–3]. To solve it, structures made of aluminum alloys were used [4, 5]. These alloys, being lightweight, strong, and corrosion-resistant, are widely used in the manufacture of welded products and structures [6, 7]. Welding aluminum alloys presents certain challenges due to their unique physical and chemical properties [8, 9]. Pulsed unipolar arc welding with a consumable electrode (hereinafter referred to as MIG welding) is one of the most promising methods for the high-performance welding of aluminum alloy structures [10, 11].

However, the MIG welding of aluminum alloys has specific characteristics that must be considered when designing welded structures and developing appropriate welding processes [12–14]. It is necessary to consider the specific thermal processes that occur during MIG welding [15–17], as well as the characteristics of residual stress-strain state formation in welded structures [18–20]. To predict physical and metallurgical processes and thermal cycles in fusion welding and related technologies, mathematical modeling methods are used [21–23]. For the distribution of residual stresses and welding deformations, numerical modeling using the finite element method is advisable, as it correlates well with experimentally measured data [24–26]. Therefore, investigating the characteristics of structure formation and residual deformation in butt and T-joints is of utmost importance [27–29]. Indeed, defects such as hydrogen porosity can arise during MIG welding of these alloys, reducing joint strength [30, 31]. The influence of welding parameters on characteristics such as hardness, tensile strength, impact toughness, and microstructure is also a significant consideration [32, 33]. Investigating this issue for relevant welded joint types will enable the optimization of parameter refinement methods based on the characteristic criteria of the resulting joint qualities [34, 35].

Of all the characteristics of welded joints mentioned, microstructure is the most interesting, as the formation of all other characteristics depends on it [36, 37]. Therefore, investigating the trends in structure formation during MIG welding of aluminum alloy butt joints at different speeds is a pertinent objective [38, 39]. Specifically, it is worthwhile to investigate the microstructure formation of the 1561 alloy within the Al-Mg-Mn system, considering its widespread use in construction and various industries [40, 41].

PURPOSE AND OBJECTIVES OF THE STUDY

This study aims to determine the trends in structure formation within welded joints of the 1561 aluminum alloy, as it is widely used for the fabrication of various domestic and industrial welded structures (e.g. marine and river vessel parts, aerospace vehicles, food and chemical industry, etc.). This will be achieved by analyzing the influence of varying MIG welding parameters, particularly welding speed and heat input, while prioritizing satisfactory seam formation. Ultimately, the goal is to identify the optimal welding parameters that minimize porosity, refine grain structure, and enhance mechanical properties.

To achieve this goal, the following tasks are proposed:

1. Conduct technological research to select MIG welding modes for butt joints of 1561 alloy on a steel backing plate. The criterion for selection is satisfactory seam formation in accordance with ISO 10042, aiming for a quality level of at least C and as close as possible to level B.
2. Conduct metallographic studies to determine the structural formation characteristics of the obtained 1561 alloy butt joints.
3. Conduct mechanical strength tests on the obtained butt joints of the 1561 alloy.
4. Establish general trends in the improvement of structure, quality, and strength of 1561 alloy joints based on the speed and heat input of the MIG welding process.

RESEARCH METHODS, MATERIALS AND EQUIPMENT

To achieve the objective of this study, the following research methodology was employed: preparation of the experimental setup, technological equipment, and welded samples. Conducting preliminary technological studies on MIG welding of 1561 aluminum alloy with a thickness of $\delta = 4$ mm, using parameters selected from literature sources (specifically, [42–44]). Experimentally refining the process parameters to achieve satisfactory seam formation as defined by the international standard ISO 10042 [45]. Achieving a seam formation quality level of at least C, and ideally approaching level B (as per ISO 10042), by utilizing various MIG welding speeds. Conducting metallographic and microhardness analyses of the butt joints produced from 1561 alloy ($\delta = 4$ mm) [46, 47]; Identifying the characteristic features of weld structure formation as a function of MIG welding speed and heat input; Performing mechanical tests to determine the strength of the produced joints [48]; Analyzing the obtained results to establish characteristic trends in structure formation and the changes in mechanical properties of 1561 alloy joints as a function of MIG welding speed and heat input.

A laboratory test bench was created based on a TPS 320i MIG/MAG welding source (Fronius International GmbH, Austria) to conduct technological research. The bench was equipped with a manipulator to move the welding torch relative to the welded samples clamped in the assembly and welding fixture (Figure 1).

Technological research on MIG welding was conducted on flat specimens of 1561 aluminum alloy (Al-Mg-Mn system) with dimensions of 300 × 100 × 4 mm (Table 1). This alloy exhibits a tensile strength of at least 360 MPa and an elongation of approximately 11%. ER5356 wire with a diameter of 1.2 mm was selected as the

Figure 1. Appearance of the laboratory test bench for conducting technological research

electrode wire (Table 1). Metallographic studies revealed that the grain size in the 1561 base metal (Ds = h × l, where Ds is grain size, h is grain width, and l is grain length) ranged from 7–10 × 20–100 µm, with a shape factor (æ = l / h) of 3–10 (Figure 2). The microhardness of the base metal was in the range of 750–840 HV.

For welding, butt-jointed samples were clamped in appropriate assembly and welding equipment. This ensured the weld root was formed using a replaceable backing bar with a forming groove. The backing, made of austenitic stainless steel, featured a 4 mm wide and 2.5 mm deep groove for weld seam root metal formation. MIG welding was conducted using high-purity (99.993%) argon shielding gas.

Metallographic studies were performed using a NEOPHOT-32 optical microscope (CARL ZEISS, Jena, Germany) following the methodology outlined in [49, 50]. To reveal the sample structures, etching was performed using an aqueous NaOH solution followed by clarification with an aqueous HNO_3 solution for macrostructure analysis. Microstructure analysis involved etching with an aqueous hydrofluoric acid solution [51, 52]. Microstructural studies were conducted following the recommendations and methodologies outlined in references [53, 54]. Vickers microhardness (HV) measurements were performed on the samples using a LECO M400 microhardness tester (St. Joseph, MI, USA) with a 100 g load. The reported hardness values represent the average of three measurements [55]. Tensile tests were conducted on a universal servohydraulic testing complex MTS 318.25 (MTS Systems Corporation, Eden Prairie, Minnesota, USA) with

Table 1. Chemical composition of the Al-Mg-Mn alloys used in the study

Material	Chemical element, wt.%									
	Al	Mg	Mn	Si	Fe	Cu	Zn	Zr	Cr	Ti
Base metal 1561	Base	5.5–6.5	0.7–1.1	≤ 0.4	≤ 0.4	≤ 0.1	≤0.2	0.02–0.12	–	–
Welding wire ER5356	Base	4.5–5.5	0.1–0.2	–	–	–	–	–	0.05–0.20	0.06–0.20

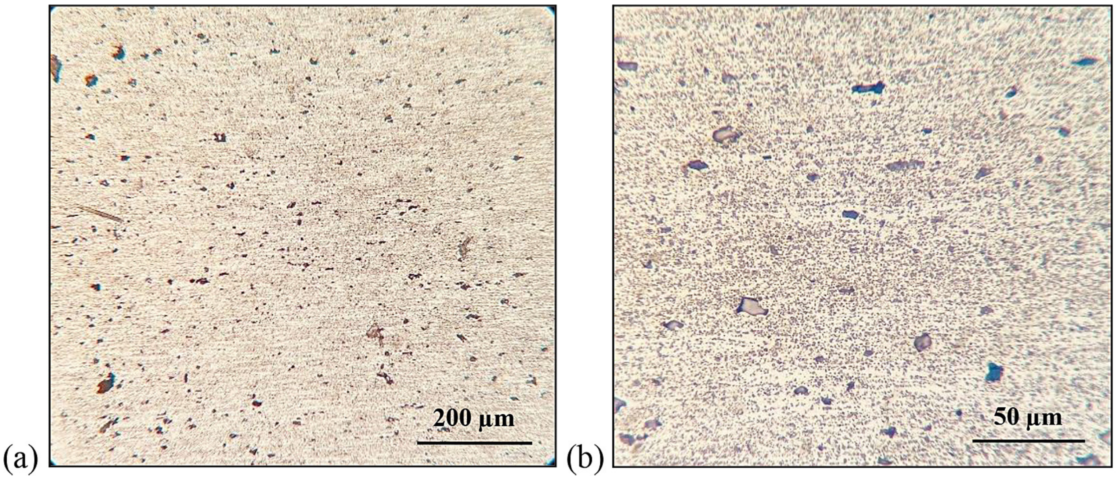

Figure 2. Microstructure of the base metal (BM) - alloy 1561: (a) ×100; (b) ×400

a maximum force of 250 kN to determine the strength of the samples. The tests were performed according to the standard method. Comprehensive material research methods were employed for all other studies [22–28].

RESULTS OF THE TECHNOLOGICAL RESEARCH ON THE MIG WELDING PROCESS OF 1561 ALLOY BUTT JOINTS

Welding parameters were selected for the study based on the recommendations of previous works [42, 43, 56, 57]. Following MIG welding experiments on butt joints of 1561 alloy specimens (300 × 100 × 4 mm) using a specifically designed laboratory bench (Figure 1), the welding parameters outlined in Table 2 were selected. Macrographs of the 1561 alloy joints produced using these MIG welding parameters are also presented in Table 2. These ground sections demonstrate satisfactory seam formation, corresponding to quality level C or B according to ISO 10042. A process efficiency of 0.8 was assumed when determining the heat input [58].

RESULTS OF THE METALLOGRAPHIC STUDIES ON THE STRUCTURE FORMATION OF BUTT JOINTS IN THE 1561 (AL-MG-MN) ALLOY

This section considers the structural formation characteristics of joints produced using three selected MIG welding modes (Table 1).

Metallographic studies of Specimen No. 1 (Figure 3, 4) revealed that the weld metal is characterized by a grain structure consisting of both equiaxed grains with sizes of Ds = 10–50 μm and elongated grains with sizes of Ds = 10–12 × 30–100 μm and a grain shape factor of æ = 3–8.3 (Table 3). The weld metal microhardness is HV 64–68 (Table 3). The weld metal is characterized by the presence of relatively large pores, with sizes of Dp = 60–230 μm (Figure 3).

The fusion line (FL) zone and heat-affected zone (HAZ) primarily exhibit elongated crystallites with sizes of Ds (h × l) = 10–30 × 30–50 μm (FL) and Ds = 7–20 × 20–100 μm (HAZ), respectively (Figure 4). The grain shape coefficient is æ = 2.7–3 (FL) and æ = 2.9–5 (HAZ).

During the transition from the weld metal to the HAZ, the equiaxed grain structure coarsens slightly (on average by a factor of 1.17, Figure 5a), while the crystallite shape coefficient (æ) decreases by an average factor of 1.4 (Figure 5b). Simultaneously, the microhardness increases by an average of 14%. The HV in the fusion line zone is practically identical to that of the weld metal.

Metallographic studies of specimen No. 2 (Figure 6, 7) determined the weld metal to have an equiaxed grain structure with a grain size of Ds = 10–60 μm (Table 4, Figure 6). Elongated grains (crystallites) are also observed, exhibiting a size of Ds = 10–15 × 30–100 μm and a grain shape factor of æ = 3–6.7. The weld metal is characterized by the presence of pores measuring Dp = 20–120 μm (Figure 6, a) and isolated inclusions up to 50 μm in size (Figure 6, b). The weld metal microhardness is HV 70–77 (Table 4).

Table 2. Welding parameters for alloy 1561 (δ = 4 mm)

No.	Wire feed speed (V_w), m/min	Average current of puls-arc welding (I), A	Puls-arc voltage, (U), V	Welding speed (V), mm/min	Linear energy input (E), J/mm	Macrosection
1.	6.9	119	15.5	380	233	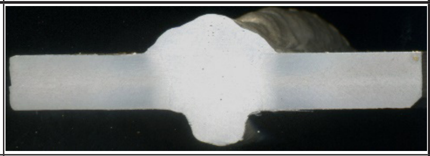
2.	8	137	18.2	500	240	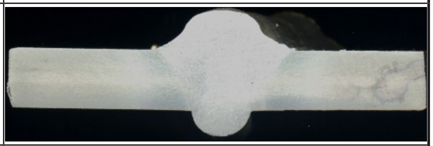
3.	8.4	142	19.1	600	220	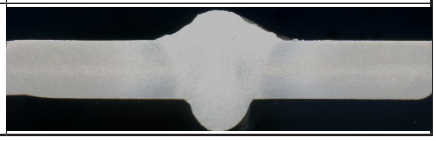

Note: The samples were welded in one pass.

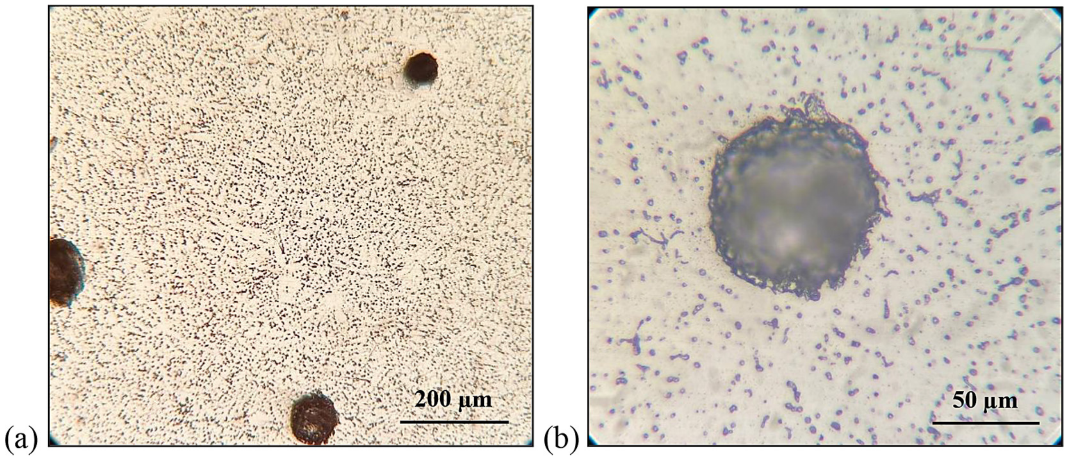

Figure 3. Microstructure of the weld metal of specimen No. 1: (a) ×100; (b) ×400

Table 3. Structural parameters of the weld metal of aluminum alloy 1561 joints, specimen No. 1

Parameters	Zones			
	Weld seam	FL	HAZ	OM
HV	64…68	66	77	74…84
Ds, µm	10…50	10…30	20…50	-
Ds (h × l), µm	10…12 × 30…100	10…30 × 30…50	7…20 × 20…100	7…10 × 20…100
æ (l / h)	3…8,3	2,7…3	2,9…5	3…10
Dp, µm	60…230	-	-	-

Note: Ds – grain size, h – crystallite width, l – crystallite length, æ – the crystallite shape factor, Dp – pore size.

Crystallites with a predominantly elongated shape are formed in the fusion line (FL) zone and the heat-affected zone (HAZ). These crystallites have sizes of Ds = 20–30 × 40–60 µm (FL) and Ds = 10–20 × 20–100 µm (HAZ), as shown in Figure 7. The grain shape factor is æ = 2 in the FL and æ = 2–5 in the HAZ. A small number of equiaxed grains are also observed, with sizes of Ds = 20–50 µm in the FL and Ds = 20–40 µm in the HAZ. The microhardness of the metal in the fusion line zone is HV 67, while in the HAZ metal it is HV 79.

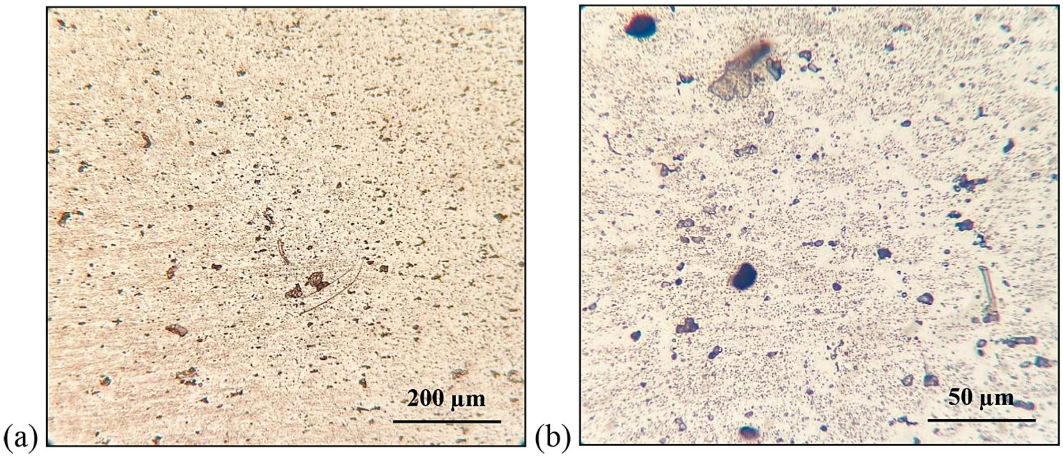

Figure 4. Metal microstructure of the fusion line (a) and HAZ (b) of the welded joint of specimen No. 1: (a) ×100; (b) ×400

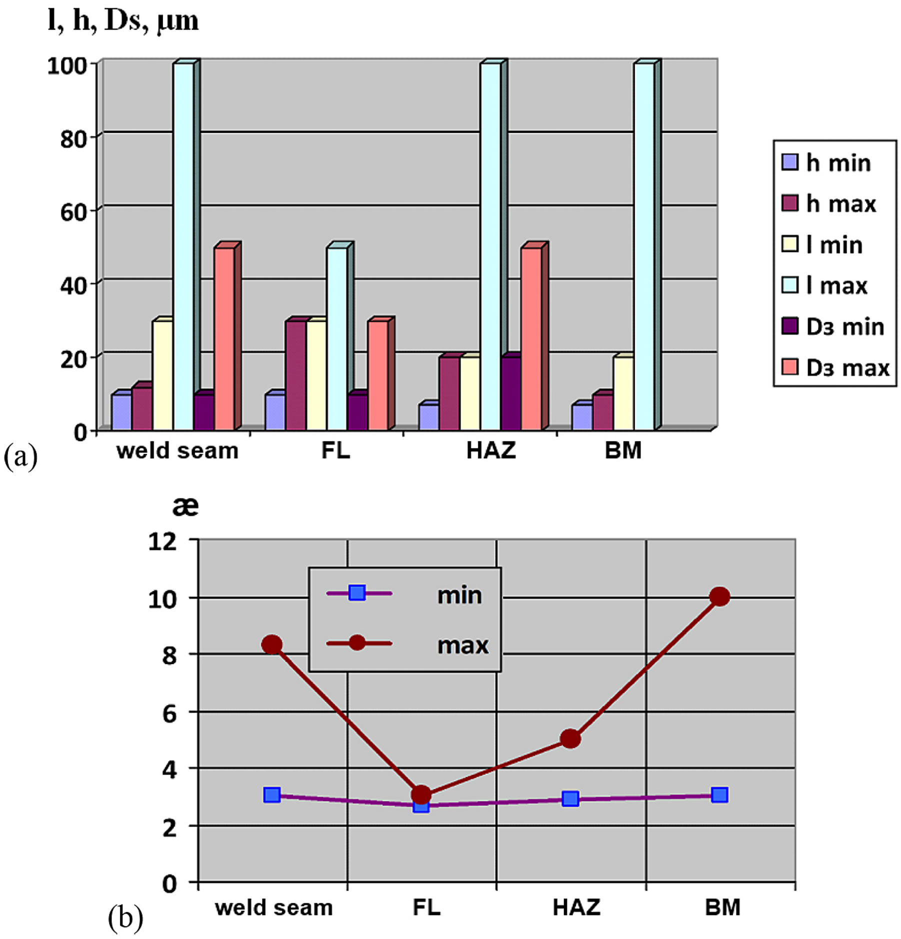

Figure 5. Change in structural parameters: h – crystallite width, l – crystallite length, Ds – grain size (a) and crystallite shape coefficient æ (b) across the zones of welded joint (weld seam, FL – fusion line, HAZ – heat-affected zone, BM – base metal) of specimen No. 1, aluminum alloy 1561.

During the transition from the weld metal to the HAZ, the equiaxed grain structure refines slightly (on average by a factor of 1.17, Figure 8a) with a decrease in the crystallite shape coefficient (æ) by an average factor of 1.4 (Figure 8b). Simultaneously, the microhardness increases slightly (by 7%); however, a decrease of 12% is observed in the fusion line zone.

Table 4. Structural parameters of the weld metal in specimen No. 2 of aluminum alloy 1561

Parameters	Zones			
	Weld seam	FL	HAZ	BM
HV	70…77	67	79	75…84
Ds, μm	10…60	20…50	20…40	-
Ds (h × l), μm	10…15 × 30…100	20…30 × 40…60	10…20 × 20…100	7…10 × 20…100
æ (l / h)	3…6,7	2	2…5	3…10
Dp, μm	20…120	-	-	-

(a) (b)
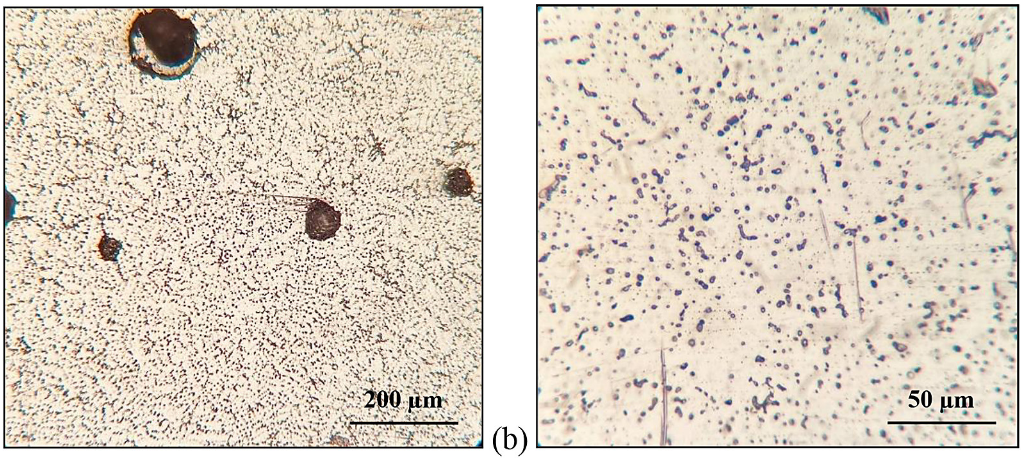

Figure 6. Microstructure of the weld metal in specimen No. 2: (a) ×100; (b) ×400

(a) (b)
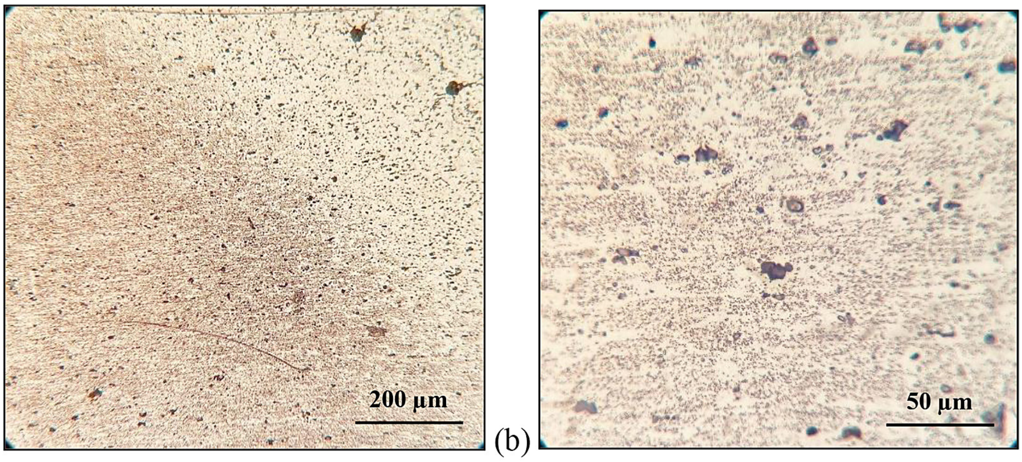

Figure 7. Microstructure of the fusion line metal (a) and HAZ (b) of the welded joint of specimen No. 2: (a) ×100; (b) ×400

Metallographic studies of specimen No. 3 (Figure 9, 10) established that the weld metal exhibited a predominantly equiaxed grain structure with a grain size (Ds) of 10–40 μm (Table 5, Figure 9). Elongated grains with a size of Ds = 10–15 × 30–70 μm and a grain shape factor of æ = 3–4.7 are also observed. The weld metal is characterized by single inclusions up to 50 μm in size (Figure 9, b). The weld metal microhardness is HV 66–78 (Table 5).

Elongated crystallites form in the fusion line (FL) zone and the heat-affected zone (HAZ), with sizes of Ds = 10–15 × 30–40 μm (FL) and Ds = 10–20 × 20–50 μm (HAZ), as shown in Figure 10. The grain shape factor is æ = 2.7–3 (FL) and æ = 2–2.5 (HAZ). A small number of equiaxed grains

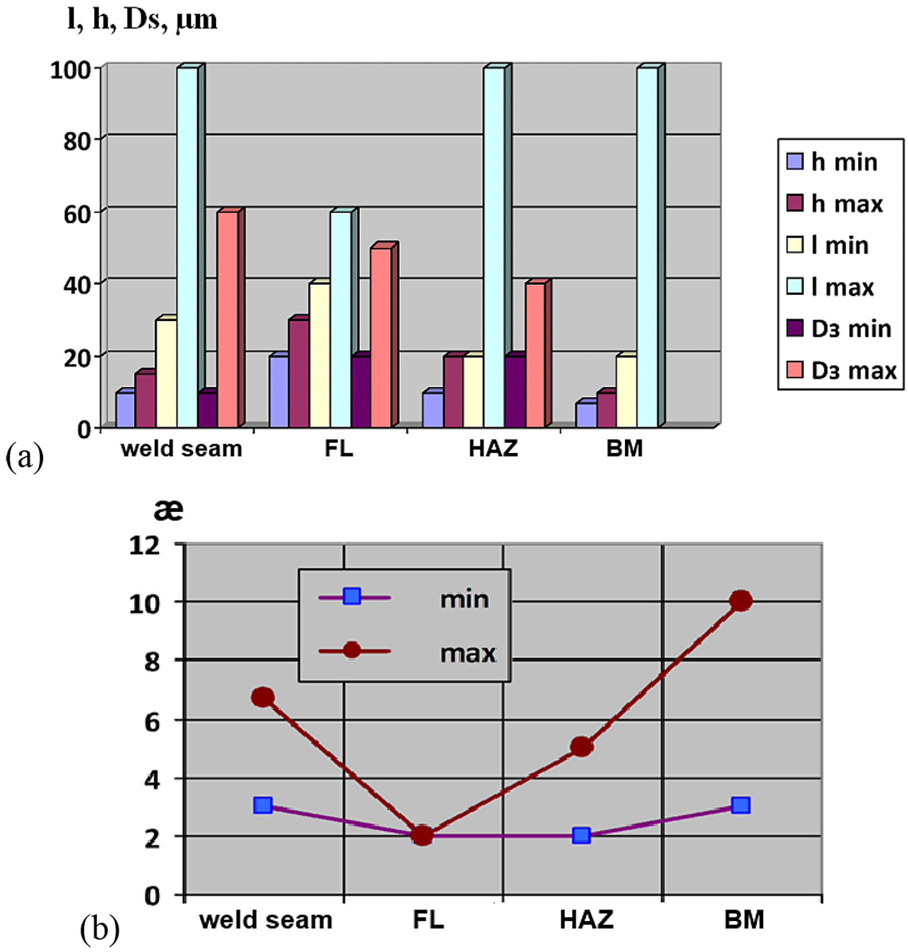

Figure 8. Changes in structural parameters: h – crystallite width, l – crystallite length, Ds – grain size (a) and crystallite shape coefficient æ (b) across the zones of the welded joint (weld seam, FL – fusion line, HAZ – heat-affected zone, OM – base metal) of specimen No. 2, aluminum alloy 1561

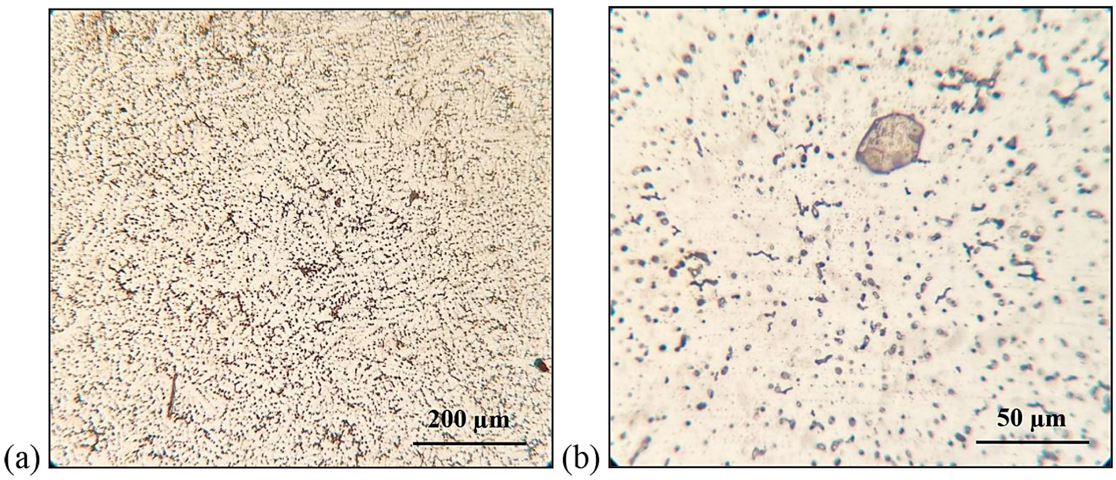

Figure 9. Metal microstructure of the weld seam in specimen No. 3: (a) ×100; (b) ×400

are also observed, measuring Ds = 15–40 µm in the FL and Ds = 15–20 µm in the HAZ. The metal microhardness is HV 65 in the fusion line zone and HV 72 in the HAZ.

The equiaxed grain structure is refined during the transition from the weld metal to the HAZ (on average by 1.4 times, Figure 11a) with a decrease in the crystallite shape coefficient (æ) by

Table 5. Structural parameters of welded joints of specimen No. 3 of aluminum alloy 1561

Parameters	Zones			
	Weld seam	FL	HAZ	OM
HV	66…78	65	72	74…80
Ds, μm	10…40	15…40	15…20	-
Ds (h × l), μm	10…15 × 30…70	10…15 × 30…40	10…20 ×20…50	7…10 × 20…100
æ (l / h)	3…4,7	2,7…3	2…2,5	3…10
Dp, μm	20…40	-	-	-

(a) (b)
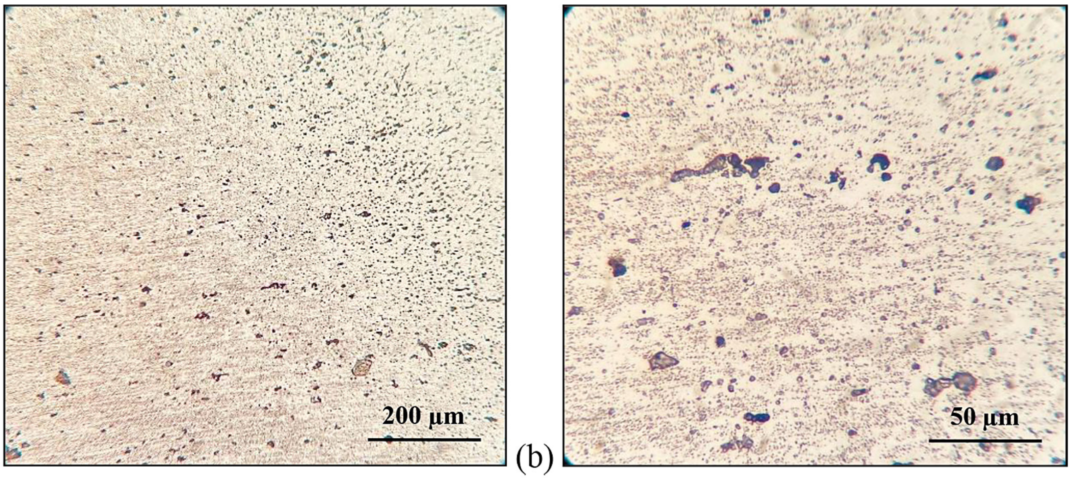

Figure 10. Microstructure of the welded joint of specimen No. 3: (a) fusion line metal at ×100 magnification; (b) HAZ at ×400 magnification

an average of 1.7 times (Figure 11b). While the microhardness changes insignificantly overall, a 10% decrease is observed in the fusion line zone.

RESULTS OF MECHANICAL TESTS OF BUTT JOINTS OF ALLOY 1561

Flat specimens, shown in Figure 12, were extracted from the welded joints and base metal for mechanical testing. In the preparation of the welded joint specimens (Figure 12b), the lower surface of the specimen was made flat by removing the weld root reinforcement. In the preparation of the welded joint specimens (Figure 12c), both the lower and upper surfaces of the specimen were made flat by removing the lower and upper weld reinforcements. A series of standard static tensile tests were conducted using a universal servo-hydraulic testing machine (MTS 318.25). The results of these tests are presented as diagrams in Figure 13. Each value on these diagrams is an average obtained from testing three specimens to failure

Mechanical testing yielded the following results. Specimen fracture occurred primarily along the fusion line. The yield and tensile strengths of welded joint specimen No. 3 were equivalent to those of the base metal. Specimen No. 2 exhibited slightly lower strength (Figure 13a). Specimen No. 1 demonstrated lower tensile strength than both specimen No. 2 and the base metal (300 MPa, Figure 13a), potentially attributable to overheating caused by the low welding speed (380 mm/min, Table 2), resulting in grain growth within the weld and HAZ. Specimen No. 1 exhibited large-diameter pores, which reduced its mechanical properties. Pore size decreased with increasing speed (Tables 3–5), but pore quantity increased.

The yield strength of the weld metal in all specimens was similar to that of the base metal. Specimen No. 1 exhibited the lowest tensile strength in its weld metal. The weld metal of specimen No. 3, welded at the highest speed and lowest linear energy, exhibited the highest strength (Table 2). Specimens No. 2 and No. 3 demonstrated the best relative elongation. The

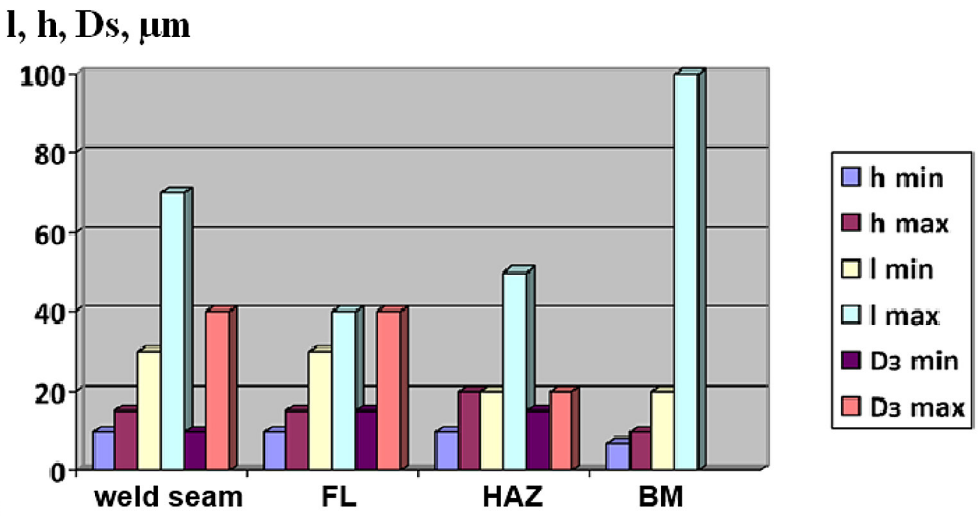

(a)

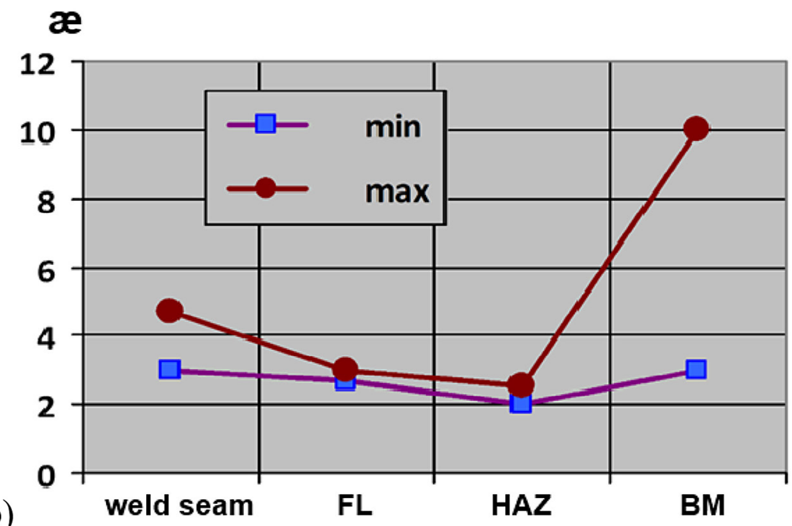

(b)

Figure 11. Change in structural parameters: h – crystallite width, l – crystallite length, Ds – grain size (a) and crystallite shape coefficient æ (b) by zones of the welded joint (weld seam, FL – fusion line, HAZ – heat-affected zone, OM – base metal) of specimen No. 3 of aluminum alloy 1561

strength coefficient, defined as the ratio of $\sigma_{0.2}$ and σ_B to OM, respectively, was smallest for specimen No. 1. Specimen No. 3 exhibited the largest strength coefficient for the weld metal. Therefore, the conducted mechanical tests indicate that MIG welding achieves optimal mechanical joint properties by reducing heat input and employing high welding speeds.

DISCUSSION OF RESEARCH RESULTS ON ALUMINUM ALLOY

The works [6-10, 15, 18, 21] show that in order to minimize welding deformations and residual stresses, as well as to improve the operational characteristics of welded structures, it is advisable to strive to achieve the formation of fine-grained weld structures. Welding Analysis reveals that samples No. 2 and No. 3 exhibit the finest grain structure (parameter Ds) within the weld metal and fusion zone. Notably, sample No. 3 displays the smallest crystallite shape coefficient (æ), as depicted in Figures 5, 8, and 11. Specimen No. 3, welded at the maximum speed and minimum linear energy of MIG welding, exhibited the largest number of pores, albeit with the smallest size (Dp) (Table 5). Pore size decreased proportionally with increasing welding speed (Tables 3–5), while pore quantity demonstrated an inverse relationship. The finest-grained weld metal structure appears in specimen No. 3. This is evident in Figure 14, which illustrates the structure and

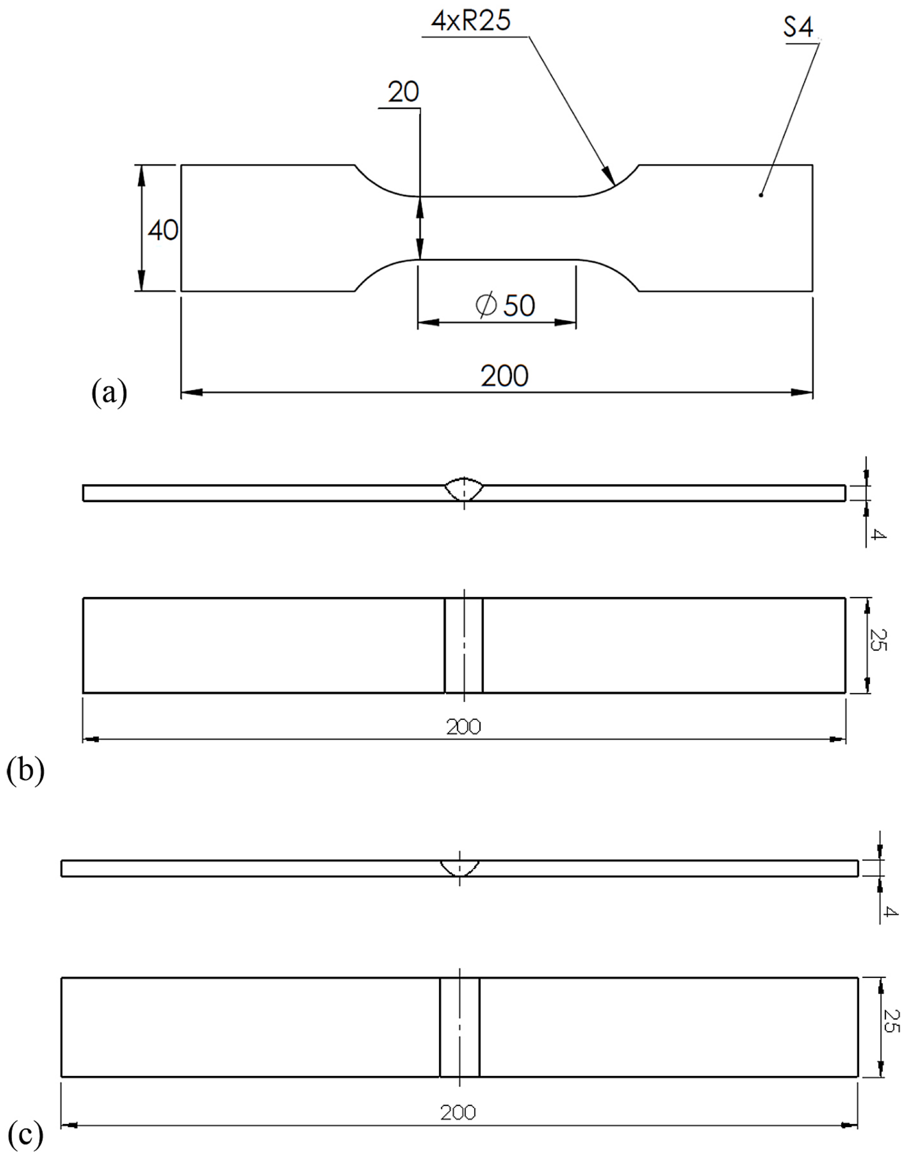

Figure 12. Shape and dimensions of the specimens for static tensile testing: (a) base metal; (b) welded joint; (c) weld metal

schematic representations of grains formed within the weld metal of the investigated 1561 aluminum alloy specimens. Therefore, according to the works [6–10, 15, 18, 21], mode No. 2 (Table 2) is preferable.

According to the work [31], when studying the microstructure of welds, it is necessary to take into account the changes in microhardness and structure at the fusion line and in the HAZ. A comparative analysis of the structural parameters across different zones (weld seam, FL, HAZ, and OM) of the welded joints revealed the following (Figure 15). In specimen No. 2, compared to specimen No. 1, increasing the MIG welding speed (Table 2) from mode No. 1 (specimen No. 1) to mode No. 2 (specimen No. 2) resulted in the following changes in the size of the equiaxed grains (Ds):

- slightly increases (by a factor of 1.17 on average) in the weld metal (Figure 15a);
- along the fusion line, D_s increases by a factor of 1.75 (Figure 15b).
- the grain structure in the HAZ metal is refined by a factor of 1.17 on average (Figure 15c).

The crystallite sizes in the weld metal, fusion lines, and HAZ are practically identical (Figure 15), with a slight decrease in their shape factor. This is in good agreement with the data of the works [11, 21, 31, 36]. Additionally, the pore sizes in the weld metal decrease by a factor of 2–3, from Dp = 60–230 μm (specimen No. 1) to

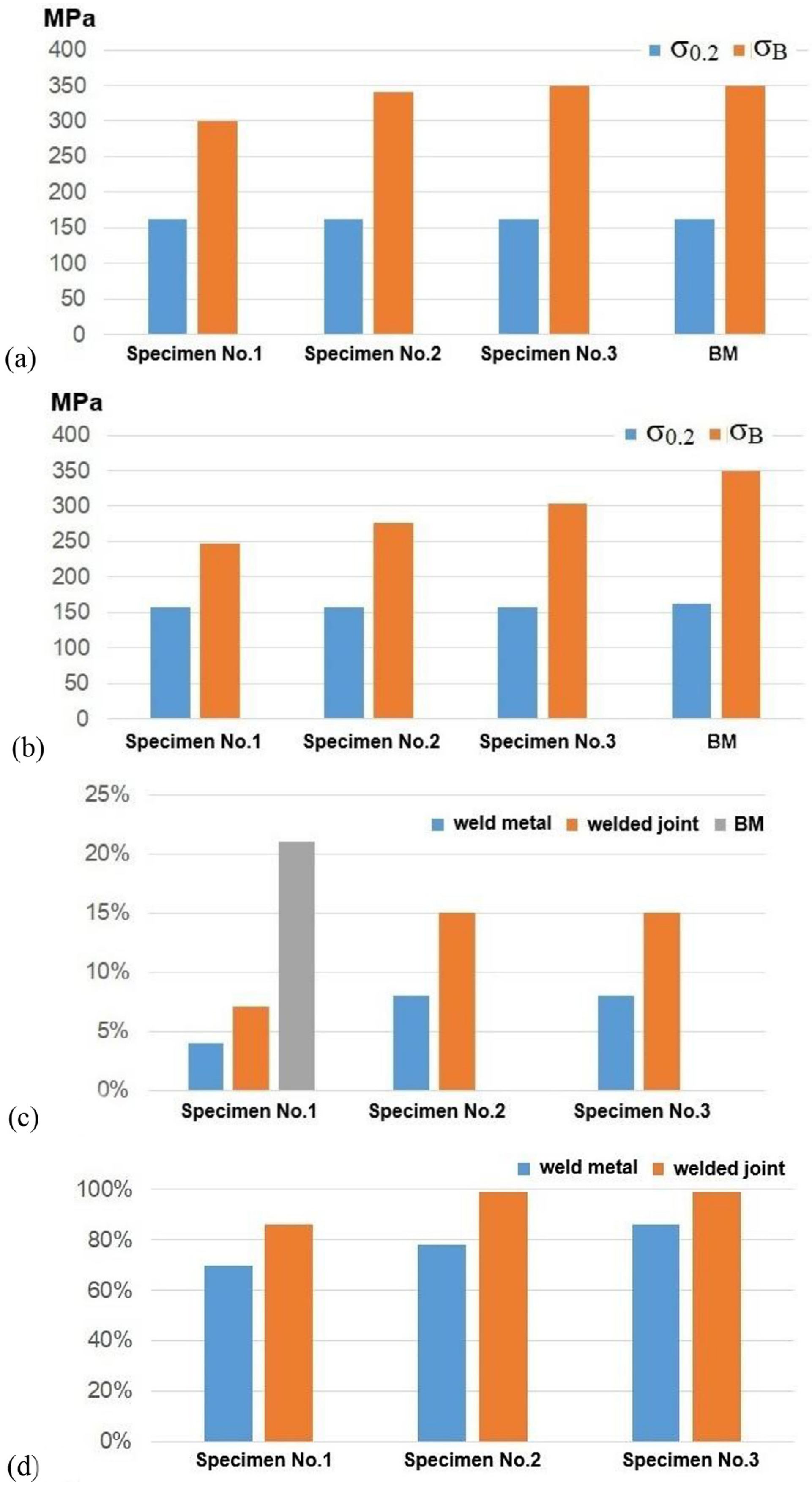

Figure 13. Results of static tensile tests of 1561 alloy specimens: (a) yield strength ($\sigma_{0.2}$) and tensile strength (σ_B) of welded joints; (b) yield strength ($\sigma_{0.2}$) and tensile strength (σ_B) of weld metal; (c) elongation; (d) strength coefficient

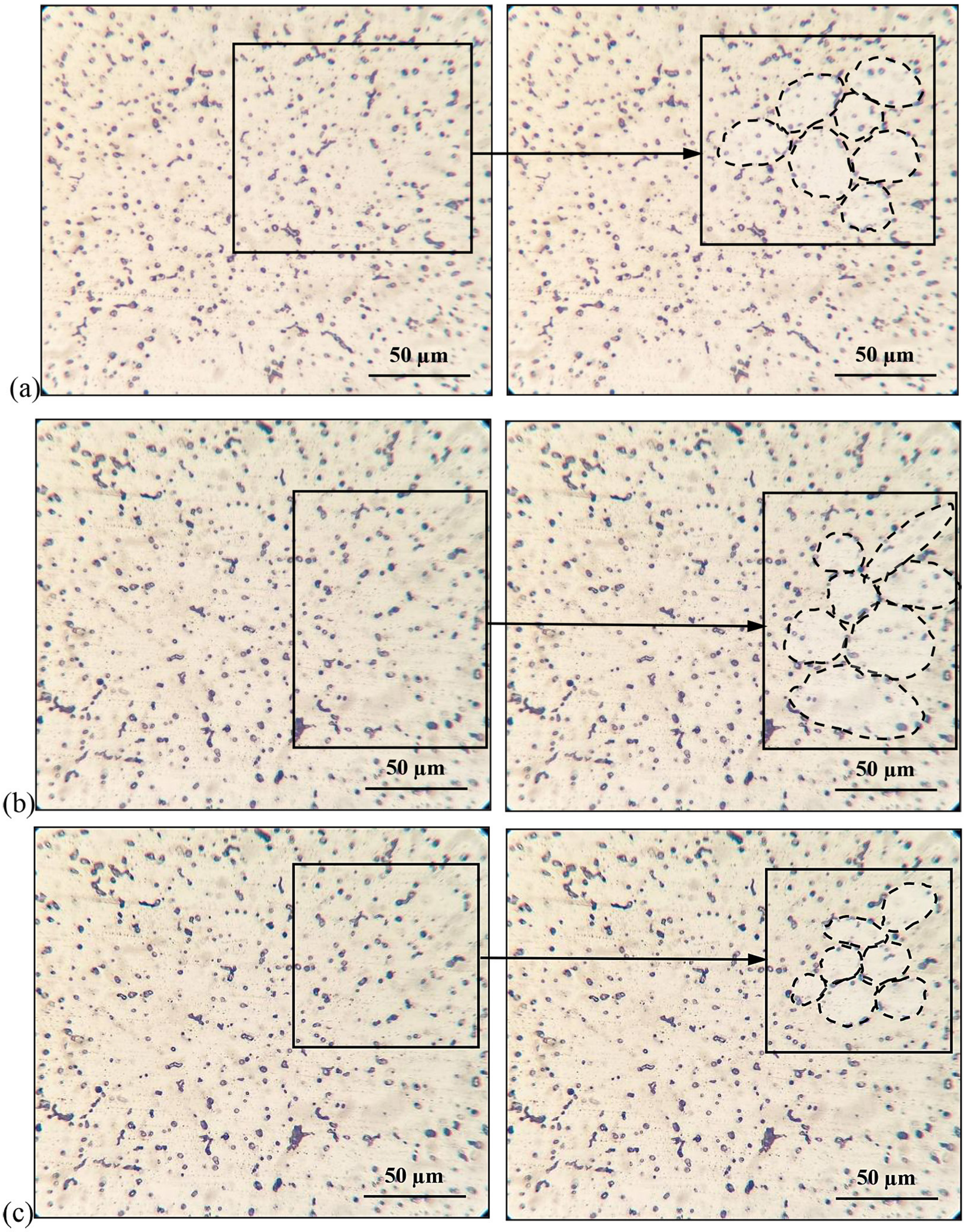

Figure 14. Microstructure of the weld seams in samples No. 1 (a), No. 2 (b), and No. 3 (c) (×400)

Dp = 20–120 µm (specimen No. 2), while their quantity increases.

A comparison of the microhardness (HV) between specimen No. 2 and specimen No. 1 revealed an 11% increase in HV for the weld metal of specimen No. 2. The HAZ metal and the fusion line exhibited approximately the same HV (Figure 16, a, b).

In sample No. 3, compared to sample No. 2, increasing the welding speed (Table 2) from mode No. 2 to mode No. 3 resulted in the following changes in the size of the equiaxed grains (Ds):

- The grain structure in the weld metal was refined by an average of 1.4 times (Figure 15a).
- The grain structure along the fusion line was refined by an average of 1.75 times (Figure 15b).

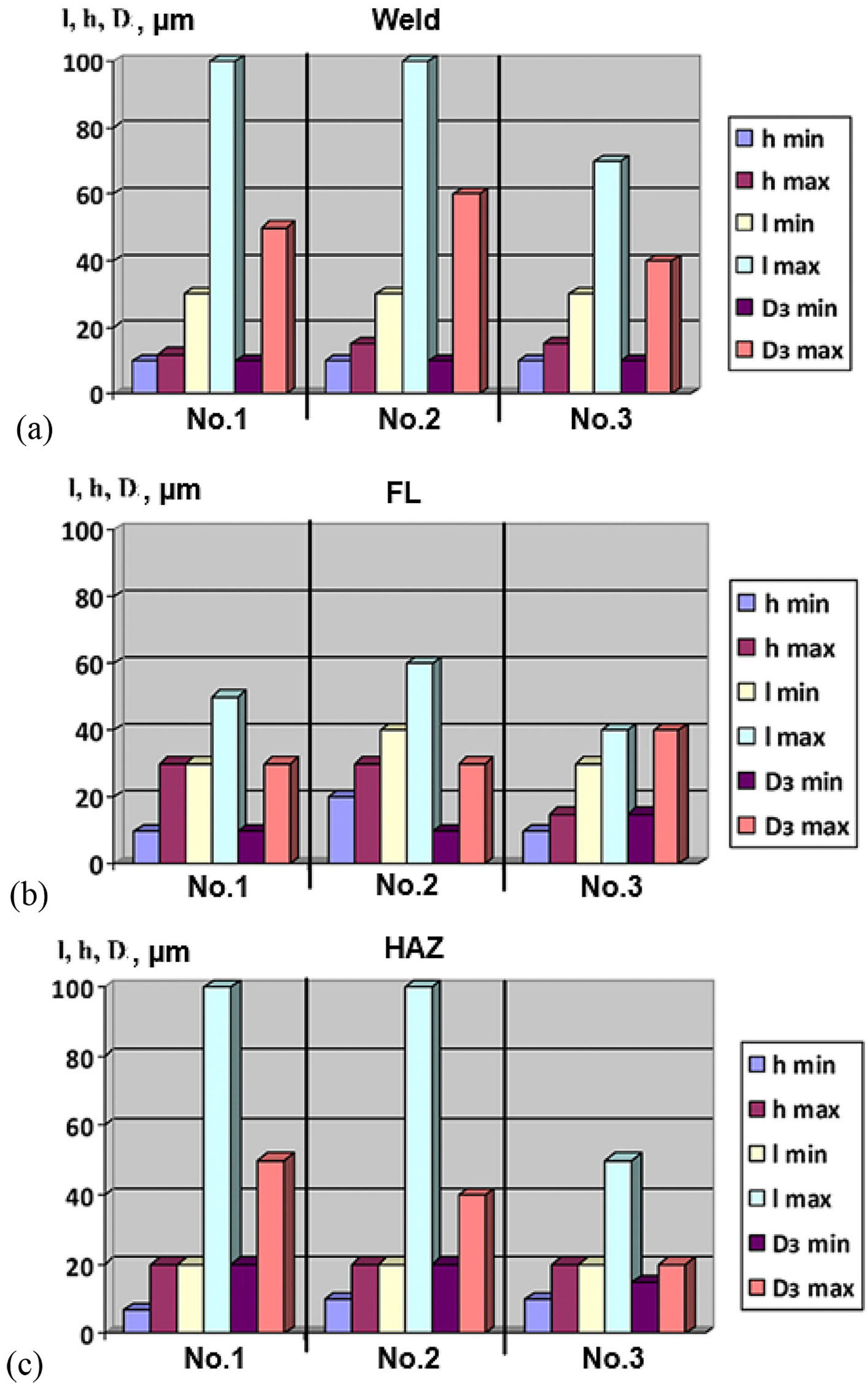

Figure 15. Change in structural parameters: h – crystallite width, l – crystallite length, D_s – grain size in the zones of the welded joint: a) in the weld metal; b) along the fusion line (FL); c) in the heat-affected zone (HAZ) of specimens No. 1, No. 2, No. 3 of aluminum alloy 1561

- The grain structure in the HAZ metal is refined by an average of 1.7 times (Figure 15, c).

Crystallite sizes in the weld and HAZ metals are significantly reduced (Figure 15) with a decrease in their shape factor. Specifically, the shape factor in the weld metal decreases from æ = 3–6.7 (specimen No. 2) to æ = 3–4.7 (specimen No. 3). in the HAZ metal, ranging from æ = 2–5 (specimen No. 2) to æ = 2–2.5 (specimen No. 3). Additionally, small

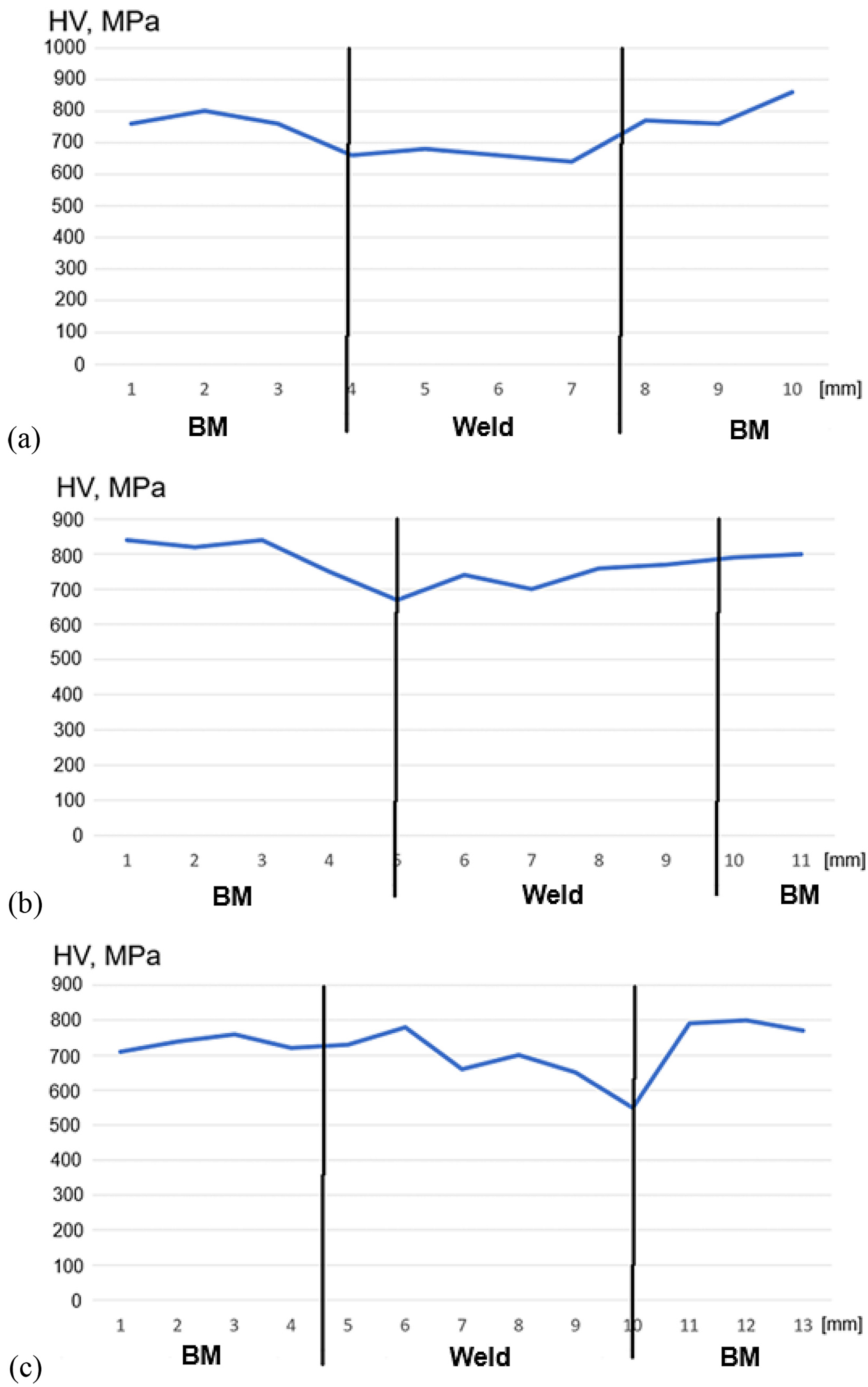

Figure 16. Change in microhardness (HV) across the cross-section of welded specimens: No. 1 (a), No. 2 (b), and No. 3 (c) of aluminum alloy 1561

pores with a size of Dp = 20–40 μm are present in the weld metal of specimen No. 3, which correlates with the data of work [30].

A comparison of the microhardness (HV) between specimen No. 3 and specimen No. 2 revealed that the HV values are approximately the same in the weld metal and along the fusion line. However, the HAZ metal of specimen No. 3 exhibits a 9% decrease in HV (Figure 16b, 16c), which correlates with the data of work [21].

Therefore, increasing the welding speed while minimizing heat input refines the structure of the 1561 aluminum alloy joint welded in mode 3 (specimen No. 3, Table 2). This refinement is characterized by a simultaneous decrease in pore size and an increase in pore quantity within the weld metal. According to work [21], such grinding contributes to an increase in strength (Figure 13). However, some fluctuations in the microhardness (HV) of specimen No. 3's weld (Figure 16, c) may slightly reduce the overall mechanical properties. Increasing the speed and minimizing the heat input is advisable for improving the joint's mechanical properties (specimen No. 3, Table 2, Figure 13). According to work [30], the disadvantage of this approach is the risk of pore formation (Dp = 20–40 μm, Table 3).

Recently, various specialized techniques have been proposed to improve the quality of welded joints of aluminum alloys obtained by MIG welding (e.g., welding in short-circuit mode [29, 40], specialized pulse modulation of the arc [39, 42], external magnetic fields [57], etc.). However, according to the authors, the correct choice of the welding mode can significantly simplify the task of improving the quality of structures made of aluminum alloys welded in industrial conditions. This opinion is also confirmed by the authors of such works as [6, 15, 27, 43]. The correct choice of the welding mode allows obtaining better results without the need to use new equipment and additional technological techniques, which has a favorable effect on the economic factors of industrial production.

Therefore, when selecting the MIG welding mode for aluminum alloy, it is advisable to maximize speed and minimize heat input while ensuring a satisfactory weld seam quality (specifically, in accordance with ISO 10042) and reliable gas shielding of the weld pool from atmospheric air. This approach can be recommended for the manufacture of welded structures from aluminum alloys used in vehicles, construction and industrial products, such as various household and industrial welded structures of sea and river vessels, aerospace technology, food and chemical industry, etc.

CONCLUSIONS

1. Technological research on selecting MIG process modes for welding butt joints of the Al-Mg-Mn alloy system (grade 1561) on a steel backing plate showed that, for satisfactory seam formation with a quality level between C and B according to ISO 10042, it is advisable to choose a speed range of 380–600 mm/min with a linear energy range of 217–240 J/mm.
2. Metallographic studies have shown that increasing the MIG welding speed of 1561 alloy butt joints to 600 mm/min, while simultaneously decreasing the heat input to 217 J/mm, contributes to weld grain refinement (Ds = 10–15 × 30–70 μm) and a decrease in the grain shape factor (æ = 3–4.7). However, this also increases the number of pores while decreasing their size (Dp = 20–40 μm). The microhardness (HV) of the weld metal increased from 640–680 MPa to 660–780 MPa when the welding speed was increased from 380 mm/min to 600 mm/min.
3. Mechanical tests conducted on butt joints of 1561 alloy revealed that increasing the heat input to 233-240 J/mm led to a deterioration in the mechanical properties of the welds, including a reduction in the weld metal strength coefficient to 70%. Increasing the MIG welding speed to 600 mm/min while simultaneously decreasing the heat input to 217 J/mm results in an observed increase in the weld metal strength coefficient to 86%. Therefore, when using MIG welding of aluminum alloys in industry, it is recommended to increase the speed to 600 mm/min and higher.

Acknowledgments

The research was funded within the following programs:

1. The GDAS'Project of Science and Technology Development [2020GDASYL-20200301001];
2. The National Key Research and Development Program of China [2020YFE0205300].
3. National Key Research and Development Program of China (Project Number: 2023YFE0201500).

REFERENCES

1. Das S., Yin W. Trends in the global aluminum fabrication industry. The Journal of The Minerals, Metals & Materials Society, 2007; 59: 83–87. https://doi.org/10.1007/s11837-007-0027-2
2. Alexopoulos N.D., Gialos A.A., Zeimpekis V., Velonaki Z., Kashaev N., Riekehr S., Karanika A. Laser beam welded structures for a regional aircraft: weight, cost and carbon footprint savings. Journal of Manufacturing Systems, 2016; 39: 38–52. https://doi.org/10.1016/j.jmsy.2016.02.002
3. Gu, Y., Zhang, W., Xu, Y. et al. Stress-assisted corrosion behaviour of Hastelloy N in FLiNaK molten salt environment // npj Mater Degrad, 2022; 6(90). https://doi.org/10.1038/s41529-022-00300-x
4. Yun X., Wang Z. Special issue editorial: Aluminium alloy structures. Structures, 2024; 69: 107297. https://doi.org/10.1016/j.istruc.2024.107297
5. Boczkal S., Mitka M., Hrabia-Wiśnios J., Płonka B., Węglowski M. St., Węglowska A., Śliwiński P. Analysis of the structure and properties of welded joints made from aluminum alloys by electron beam welding (EBW) and friction stir welding (FSW). Crystals, 2025; 15(3): 208. https://doi.org/10.3390/cryst15030208
6. Chen B.-Q., Liu K., Xu S. Recent advances in aluminum welding for marine structures. Journal of Marine Science and Engineering, 2024; 12(9): 1539. https://doi.org/10.3390/jmse12091539
7. Kuchuk-Yatsenko S.I., Hushchyn K.V., Ziakhor I.V., Samotryasov S.M., Zavertannyi M.S. and Levchuk A.M. Structure and mechanical properties of 2219-T87 aluminium alloy joints produced by flash butt welding, The Paton Welding Journal, 2021; 8: 27–32. https://doi.org/10.37434/tpwj2021.08.06
8. Olabode M., Kah P., Martikainen J. Aluminium alloys welding processes: Challenges, joint types and process selection. Proceedings of the Institution of Mechanical Engineers, Part B, Journal of Engineering Manufacture, 2013; 227: 1129–1137. https://doi.org/10.1177/0954405413484015
9. Verma R.P., Pandey K.N., András K., Khargotra R., Singh T. Difficulties and redressal in joining of aluminium alloys by GMA and GTA welding: a review. Journal of Materials Research and Technology, 2023; 23: 2576–2586. https://doi.org/10.1016/j.jmrt.2023.01.183
10. Ramji B.R., Bharathi V., Prabhu Swamy N.R. Characterization of TIG and MIG welded aluminium 6063 alloys. Materials Today: Proceedings, 2021; 46(18): 8895–8899. https://doi.org/10.1016/j.matpr.2021.05.356
11. Ye M., Wang Z., Butt H. A., Yang M., Chen H., Han K., Cui M., Lei Y. Enhancing the joint of dissimilar aluminum alloys through MIG welding approach assisted by ultrasonic frequency pulse. Materials Letters, 2023; 330: 133289. https://doi.org/10.1016/j.matlet.2022.133289
12. Prokopov, V., Fialko, N., Sherenkovskaya, G. et al. Effect of the coating porosity on the processes of heat transfer under, gas-thermal atomization. Powder Metall. Met. Ceram. 1993; (32): 118–121. https://doi.org/10.1007/BF00560034
13. Fialko, N., Prokopov, V., Meranova, N. et al. Thermal physics of gas thermal coatings formation processes. State of investigations. Fizika i Khimiya Obrabotki Materialov, 1993; 4: 83–93.
14. Tsybulkin G.A. Study of pulsed arc processes at periodic switching of volt-ampere characteristics of arc power source. The Paton Welding Journal, 2019; 7: 2–6. https://doi.org/10.15407/tpwj2019.07.01
15. Sevim I., Hayat F., Kaya Y., Kahraman N. The study of MIG weldability of heat-treated aluminum alloys. The International Journal of Advanced Manufacturing Technology, 2012; 66(9–12). https://doi.org/10.1007/s00170-012-4462-z
16. Fialko, N., Prokopov, V., Meranova, N. et al. Temperature conditions of particle-substrate systems in a gas-thermal deposition process. Fizika i Khimiya Obrabotki Materialov, 1994; 2: 59–67.
17. Zhu S., Wang Q., Yin F., Liang Y., Wang X. Research on Thermal Process of MIG Welding of Aluminum Alloy with Longitudinal Magnetic Field. The Open Mechanical Engineering Journal, 2011; 5: 32–38. https://doi.org/10.2174/1874155X01105010032
18. Schubert E. Challenges in thermal welding of aluminium alloys. World Journal of Engineering and Technology, 2018; 6(2): 296–303. https://doi.org/10.4236/wjet.2018.62018
19. Prokopov, V.G., Fialko, N.M., Sherenkovskaya, G.P. et al. Effect of coating porosity on the process of heat transfer with gas-thermal deposition. Powder Metall Met Ceram 1993; 32: 118–121. https://doi.org/10.1007/BF00560034
20. Leggatt R.H. Residual stresses in welded structures. International Journal of Pressure Vessels and Piping, 2008; 85(3): 144–151. https://doi.org/10.1016/j.ijpvp.2007.10.004
21. Peel M., Steuwer A., Preuss M., Withers P.J. Microstructure, mechanical properties and residual stresses as a function of welding speed in aluminium AA5083 friction stir welds. Acta Materialia, 2003; 51(16): 4791–4801. https://doi.org/10.1016/S1359-6454(03)00319-7
22. Fialko, N.M., Prokopov, V.G., Meranova, N.O. et al. Temperature conditions of particle-substrate systems in a gas-thermaldeposition process. Fizika i Khimiya Obrabotki Materialov, 1994; 2: 59–67.
23. Kvasnytskyi V., Korzhyk, V., Kvasnytskyi V.,

Mialnitsa H., Dong C., Pryadko T., Matviienko M., Buturlia Y. Designing brazing filler metal for heat-resistant alloys based on NI3AL intermetallide. Eastern-European Journal of Enterprise Technologies. 2020; 6(108): 6–19. https://doi.org/10.15587/1729-4061.2020.217819

24. Mao D., Xie Y., Meng X., Ma X., Zhang Z., Sun X., Wan L., Volodymyr K., Huang Y. Strength-ductility materials by engineering a coherent interface at in coherent precipitates. Materials Horizons, 2024; 11(14): 3408–3419. https://doi.org/10.1039/D4MH00139G
25. Fialko N.M., Prokopov V.G., Meranov N.O., Borisov Yu.S., Korzhik V.N., Sherenkovskaya G.P. Temperature conditions of particle-substrate systems in a gas-thermal deposition process. Fizika i Khimiya Obrabotki Materialov, 1994; 2: 59–67.
26. Fialko N., Prokopov V., Meranov N. et al. Thermal physics of gas-thermal coatings formation processes. State of investigations. Fizika i Khimiya Obrabotki Materialov, 1993; 4: 83–93.
27. Lu Y., Zhu S., Zhao Z., Chen T., Zeng J. Numerical simulation of residual stresses in aluminum alloy welded joints. Journal of Manufacturing Processes, 2020; 50: 380–393. https://doi.org/10.1016/j.jmapro.2019.12.056
28. Fialko, N., Dinzhos, R., Sherenkovskii, J. et al. Establishment of regularities of influence on the specific heat capacity and thermal diffusivity of polymer nanocomposites of a complex of defining parameters. Eastern-European Journal of Enterprise Technologies. 2021; (114): 34–39. https://doi.org/10.15587/1729-4061.2021.245274
29. Nishimura R., Ma N., Liu Y., Li W., Yasuki T. Measurement and analysis of welding deformation and residual stress in CMT welded lap joints of 1180 MPa steel sheets. Journal of Manufacturing Processes, 2021; 72: 515–528. https://doi.org/10.1016/j.jmapro.2021.10.050
30. Ardika R. D., Triyono T., Muhayat N., Triyono A review porosity in aluminum welding. Procedia Structural Integrity, 2021; 33: 171–180. https://doi.org/10.1016/j.prostr.2021.10.021
31. Nie F., Dong H., Chen S., Li P., Wang L., Zhao Z., Li X., Zhang H. Microstructure and Mechanical Properties of Pulse MIG Welded 6061/A356 Aluminum Alloy Dissimilar Butt Joints. Journal of Materials Science & Technology, 2018; 34(3): 551–560. https://doi.org/10.1016/j.jmst.2016.11.004
32. Sevim I., Hayat F., Kaya Y., Kahraman N., Şahin S. The study of MIG weldability of heat-treated aluminum alloys. The International Journal of Advanced Manufacturing Technology, 2013; 66: 1825–1834. https://doi.org/10.1007/s00170-012-4462-z
33. Korzhik V.N. Theoretical analysis of amorphization conditions for metallic alloys under gas-thermal spraying. III. Transformations in the amorphized alloy underbuilding-up of coatings. Poroshkovaya Metallurgiya, 1992; 11: 47–52.
34. Jing H., Shi, Y., Gang Zh., Volodymyr K., Le W.-Y. Minimizing defects and controlling the morphology of laser welded aluminum alloys using power modulation-based laser beam oscillation. J. Manufacturing Processes. 2022; 83: 49–59. http://dx.doi.org/10.1016/j.jmapro.2022.08.031
35. Gu Y., Xu Y., Shi Y., Feng C., Volodymyr K. Corrosion resistance of 316 stainless steel in a simulated pressurized waterreactor improved by laser cladding with chromium. Surface and Coatings Technology, 2022; 441: 128534. https://doi.org/10.1016/j.surfcoat.2022.128534
36. Pan D., Pan Q., Yu Q., Li G., Liu B., Deng Y., Liu H. Microstructure and fatigue behavior of MIG-welded joints of 6005A aluminum alloy with trace amounts of scandium. Materials Characterization, 2022; 194: 112482. https://doi.org/10.1016/j.matchar.2022.112482
37. Fialko N., Dinzhos R., Sherenkovskaya G., Lazarenko M., Makhrovskyi V. Influence on the thermophysical properties of nanocomposites of the duration of mixing of components in the polymer melt. Eastern-European Journal of Enterprise Technologies, 2022; 2(5–116): 25–30. https://doi.org/10.15587/1729-4061.2022.255830
38. Liu S., Liu Z., Wang H., Liang J., Zhu X. Study on microstructure and mechanical properties of 5052 aluminum alloy MIG welded joint for high-speed train. Materials Research Express, 2024; 11(8): 086507. https://doi.org/10.1088/2053-1591/ad6b01
39. Yi J., Cao S.-F., Li L.-X., Guo P.-C., Liu K.-Y. Effect of welding current on morphology and microstructure of Al alloy T-joint in double-pulsed MIG welding. Transactions of Nonferrous Metals Society of China, 2015; 25(10): 3204–3211. https://doi.org/10.1016/S1003-6326(15)63953-X
40. Han S. G., Zheng S. D., Cai D. T., Yi Y. Y., Luo Z. Y. Microstructure characteristics and properties of 1561 aluminum alloy weldments processed by different MIG welding. Materials Science Forum, 2017; 893: 163–168. https://doi.org/10.4028/www.scientific.net/MSF.893.163
41. Skorokhod A.Z., Sviridova I.S., Korzhik V.N. Structural and mechanical properties of polyethylene terephthalatecoatings as affected by mechanical pretreatment of powder in thecourse of preparation. Mekhanika Kompozitnykh Materialov, 1994; 30(4): 455–463.
42. Zhernosekov A., Fedorchuk V., Novomlynets O. Regulation of current pulse parameters during MIG welding of aluminum alloys. Technical sciences and technologies, 2022; 2(28): 31–37. https://doi.org/10.25140/2411-5363-2022-2(28)-31-37
43. Nie J., Meng X.-F., Shi Y. Study on evaluation

method of aluminum alloy pulse MIG welding stability based on arc voltage probability density, Journal of Signal and Information Processing, 2011; 2(3): 159–164. https://doi.org/10.4236/jsip.2011.23020

44. Borisov Yu.S., Kunitskii Yu.A., Korzhik V.N., Yaprakova M.G. Structure and some physical properties of plasma-sprayed coatings of thenickel boride NiB. Soviet Powder Metallurgy and Metal Ceramics, 1986; 25(12): 966–969.
45. ISO 10042:2018. Welding – Arc-welded joints in aluminium and its alloys — Quality levels for imperfections. Access mode: https://www.iso.org/standard/70566.html
46. Mohammadtaheri M. A New metallographic technique for revealing grain boundaries in aluminum alloys. Metallography Microstructure and Analysis, 2012; 1(5): 224–226. https://doi.org/10.1007/s13632-012-0033-9
47. Lin C.-W., Hung F.-Y., Lui T.-S. Microstructure evolution and microstructural characteristics of Al–Mg–Si aluminum alloys fabricated by a modified strain-induced melting activation process. Metals, 2018; 8(1): 3. https://doi.org/10.3390/met8010003
48. Tanaka T., Morishige T., Hirata T. Comprehensive analysis of joint strength for dissimilar friction stir welds of mild steel to aluminum alloys. Scripta Materialia, 2009; 61(7): 756–759. https://doi.org/10.1016/j.scriptamat.2009.06.022
49. Standard Guide for Preparation of Metallographic Specimens (2011). Copyright © ASTM International, 100 Barr Harbor Drive, PO Box C700, West Conshohocken, PA 19428-2959. United States. https://doi.org/10.1520/E0003-11
50. Skorokhod A.Z., Sviridova I.S., Korzhik V.N. The effect of mechanical pretreatment of polyethylene terephthalate powderon the structural and mechanical properties of coatings made from it. Mechanics of Composite Materials, 1995; 30(4): 328–334. https://doi.org/10.1007/BF00634755
51. Mohammadtaheri M. A New Metallographic Technique for Revealing Grain Boundaries in Aluminum Alloys. Metallography Microstructure and Analysis, 2012; 1: 224–226. https://doi.org/10.1007/s13632-012-0033-9
52. Fialko N., Dinzhos R., Sherenkovskii J., Meranova N., Aloshko S., Izvorska D., Korzhyk V., Lazarenko M., Mankus I., Nedbaievska L. Establishment of regularities of influence on the specific heat capacity and thermal diffusivity of polymer nanocomposites of a complex of defining parameters. Eastern-European Journal of Enterprise Technologies, 2021; 6(12(114)): 6–12. http://dx.doi.org/10.15587/1729-4061.2021.245274
53. Čičo P., Kalincová D., Kotus M. Influence of welding method on microstructural creation of welded joints. Research in Agricultural Engineering, 2011; 57(Special Issue). http://dx.doi.org/10.17221/57/2010-RAE
54. Fialko N., Dinzhos R., Sherenkovskii J., Meranova N., Korzhyk V., Lazarenko M., Koseva N. Establishing patterns in the effect of temperature regime when manufacturing nanocomposites on their heat-conducting properties. Eastern-European Journal of Enterprise Technologies, 2021; 4(5(112)): 21–26. http://dx.doi.org/10.15587/1729-4061.2021.236915
55. Akca E., Trgo E. Metallographic procedures and analysis – A review. Periodicals of Engineering and Natural Sciences (PEN), 2015; 3(2): 9–11. https://doi.org/10.21533/pen.v3i2.51
56. Yasuda K. MIG welding of aluminium alloys. Welding International, 1991; 5(8): 614–617. https://doi.org/10.1080/09507119109446786
57. Wu L., Han X., Wu X., Wu Y., Chen J., Su H., Wu C. The study of high-speed MIG welding assisted by compound external magnetic fields for 6N01-T6 aluminum alloy. Journal of Manufacturing Processes, 2022; 83: 576–589. https://doi.org/10.1016/j.jmapro.2022.09.028
58. Pépe N., Egerland S., Colegrove P. A., Yapp D., Leonhartsberger A., Scotti A. Measuring the process efficiency of controlled gas metal arc welding processes. Science and Technology of Welding and Joining, 2011; 16(5): 412–417. https://doi.org/10.1179/1362171810Y.0000000029